

Jillian R.A. Newton¹, Narciso Couto², Jill Barber², Richard Bojar³, James Sidaway⁴ and Malcolm R Clench¹
¹Sheffield Hallam University U.K., ²University of Manchester U.K., ³Innovenn Ltd York UK, ⁴Phenotox Ltd, Bollington UK

Overview

- An untargeted proteomic analysis of two preparations of a commercial living skin equivalent (LSE) and human skin samples from five female donors and one male donor has been carried out. The skin samples were all taken from healthy individuals undergoing routine surgery. Analysis of the proteomics results found approximately 50 phase I and II XMEs and transporters in the LSE and the data was comparable to that obtained from the ex vivo human skin .
- Since the levels of XMEs were low in order to study their distribution a methodology for substrate based mass spectrometry imaging was developed based on MALDI-MS. Initial experiments optimised a method for applying the MALDI matrix by sublimation. Pilot studies then assessed the metabolism of four different XME substrates by SB-MSI in the LSE.

Introduction

Current animal-free approaches for assessing the metabolism of xenobiotics in skin are limited. The primary reason for this is that the levels and distribution of xenobiotic metabolising enzymes in skin are not well characterised¹. The overall aim of this project was to develop a combined *in silico-in vitro* system for predicting xenobiotic metabolism in human skin from experiments carried out on a living skin equivalent (LSE). In order to do this it was required to systematically quantify the level of xenobiotic metabolising enzymes in skin and in Labskin using proteomics. In order to examine the distribution of enzymes detected a novel substrate-based mass spectrometry imaging technique was proposed that would allow the activity of xenobiotic metabolising enzymes to be localised within the in vitro model. Ultimately the project will use these proteomic and imaging data to build a pharmacokinetic based pharmacokinetic (PBPK) model of human skin xenobiotic metabolism and disposition to enable in vitro to in vivo extrapolation (IVIVE) of LSE based xenobiotic metabolism data. This integrated solution would then offer an animal-free alternative that will increase screening capacity and knowledge of xenobiotic skin metabolism.

Material and Methods

- (i) *Samples*: Human skin was provide by the Human Tissue Bank at the University of Bradford. Samples were collected with informed ethical consent during routine surgery. Samples of the commercial full thickness living skin equivalent model "Labskin" were supplied by Innovenn Ltd (York UK).
- (ii) *Proteomics*: Human skin and Labskin samples were homogenised and treated with detergent; debris was removed. The crude fraction was ultra centrifuged, cytosolic fraction was collected. For two liver samples and one skin sample the pellet (microsomes) were resuspended detergent-based buffer and further ultra centrifuged to separate soluble and membrane fractions. The FASP method was used to digest the samples, whereas van Eijl et al¹ used a gel-based method. Mass spectrometry was performed on an Orbitrap HF instrument, with label-free quantification and peptide identification, using Progenesis QIP.
- (iii) *SB-MSI*: SB-MSI probes: Terbinafine, tolbutamide, methyl-paraben and benzydamine were applied to the surface of Labskin in an acetone:olive oil delivery system. After incubation for 48 hours samples were snap frozen and cryosectioned (12 µm) . Matrix (αCHCA) was applied by sublimation prior to imaging on a Bruker Autoflex III MALDI-Tof-Tof.

Family	Protein Name	Labskin 05	Labskin 06	Human Skin 07	Human Skin 52	Human Skin 56	Human Skin 57	Human Skin 58	Human Skin 60
Aldo-keto reductase	Aldo-keto reductase 1A1	ND	2.1	1.3	ND	ND	3.8	5.0	ND
Aldo-keto reductase	Aldo-keto reductase 1B1	ND	0.9	1.9	2.9	ND	4.3	2.4	6.5
Aldo-keto reductase	Aldo-keto reductase 1C1	ND	ND	8.3	66.1	ND	257.9	ND	ND
Aldo-keto reductase	Aldo-keto reductase 1C2	ND	ND	ND	ND	ND	20.6	ND	ND
Aldo-keto reductase	Aldo-keto reductase 1C4	ND	ND	ND	78.6	ND	ND	ND	81.8
Aldo-keto reductase	Aldo-keto reductase 7A2	ND	ND	ND	ND	ND	ND	ND	5.3
Aldehyde dehydrogenase	Aldehyde dehydrogenase 1A1	ND	2.4	9.2	12.9	ND	19.8	6.3	18.9
Aldehyde dehydrogenase	Aldehyde dehydrogenase 1B1	ND	ND	ND	ND	ND	ND	48.2	ND
Aldehyde dehydrogenase	Aldehyde dehydrogenase 1L1	ND	ND	ND	ND	26.3	ND	ND	ND
Aldehyde dehydrogenase	Aldehyde dehydrogenase 1L2	2.5	ND	ND	ND	156.1	ND	ND	ND
Aldehyde dehydrogenase	Aldehyde dehydrogenase 2	ND	2.1	12.6	10.7	ND	18.0	8.3	19.9
Aldehyde dehydrogenase	Aldehyde dehydrogenase 3A1	ND	0.6	ND	ND	ND	6.6	ND	3.5
Aldehyde dehydrogenase	Aldehyde dehydrogenase 7A1	1.7	ND	ND	ND	ND	ND	3.2	24.1
Aldehyde dehydrogenase	Aldehyde dehydrogenase 4A1	1.6	ND	ND	ND	ND	ND	ND	ND
Aldehyde dehydrogenase	Aldehyde dehydrogenase 9A1	3.8	1.3	6.6	4.1	8.0	10.2	27.9	14.2
Esterase	Carboxylesterase 1	ND	0.3	15.3	17.3	ND	6.3	2.6	19.0
Hydrolase	S-formylglutathione hydrolase (Esterase D)	2.6	4.5	14.7	14.1	7.7	19.5	14.4	22.2
Hydrolase	Leukotriene A-4 hydrolase	ND	0.7	1.5	3.2	ND	4.0	ND	7.6
Hydrolase	Epoxide hydrolase	2.2	ND	ND	ND	ND	ND	ND	6.0
Hydrolase	Bifunctional epoxide hydrolase 2	1.5	ND	ND	ND	ND	ND	ND	ND
Monoamine oxidase	Membrane primary amine oxidase	ND	9.2	4.5	16.2	ND	44.6	67.7	63.3
Monoamine oxidase	Retina-specific copper amine oxidase (AOC2)	ND	ND	3.3	ND	ND	ND	ND	ND
Other reductase	Biliverdin reductase A	ND	0.8	ND	ND	ND	ND	ND	ND
Synthase	Prostaglandin G/H synthase 1	2.1	ND	ND	ND	ND	ND	ND	ND

Table 1: expression of soluble phase I XMEs in Labskin and human skin. Orange colouring indicates consistency in expression between in vitro and in vivo samples and magnitude of expression. All data is fmol/ug. ND is not detected, NQ is not quantified

Protein Name	labskin 05	labskin 06	Human Skin 07	Human Skin 52	Human Skin 56	Human Skin 57	Human Skin 58	Human Skin 60
Catechol O-methyltransferase (EC 2.1.1.6)	6.1	0.8	ND	ND	7.2	ND	ND	NQ
Glutathione S-transferase P1-1	56.3	22.7	50.8	54.5	65.3	150.2	137.7	129.1
Glutathione S-transferase Mu 5	ND	5.2	ND	88.0	ND	12.1	ND	NQ
Glutathione S-transferase theta-1	ND	1.3	3.3	ND	ND	ND	ND	NQ
Glutathione S-transferase Mu 1	ND	NQ	ND	ND	ND	NQ	ND	2.9
Glutathione S-transferase Mu 2	ND	NQ	2.1	ND	ND	NQ	ND	22.9
Glutathione S-transferase Mu 4	ND	ND	ND	ND	ND	46.6	ND	ND

Table 2: expression of soluble phase II XMEs in Labskin and human skin. Orange colouring indicates consistency in expression between in vitro and in vivo samples and magnitude of expression. All data is fmol/ug

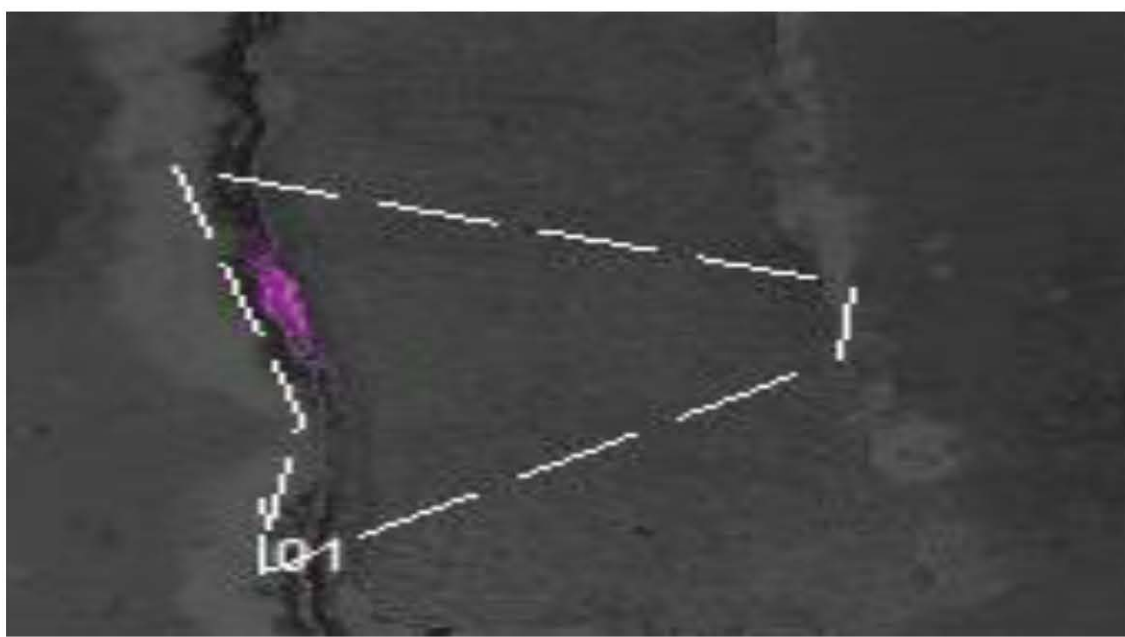


Figure 1: Optimised SB-MSI experiment on Terbinafine (purple) a substrate for CYP2C9, CYP1A2, and CYP3A4 no evidence of metabolite formation was observed.

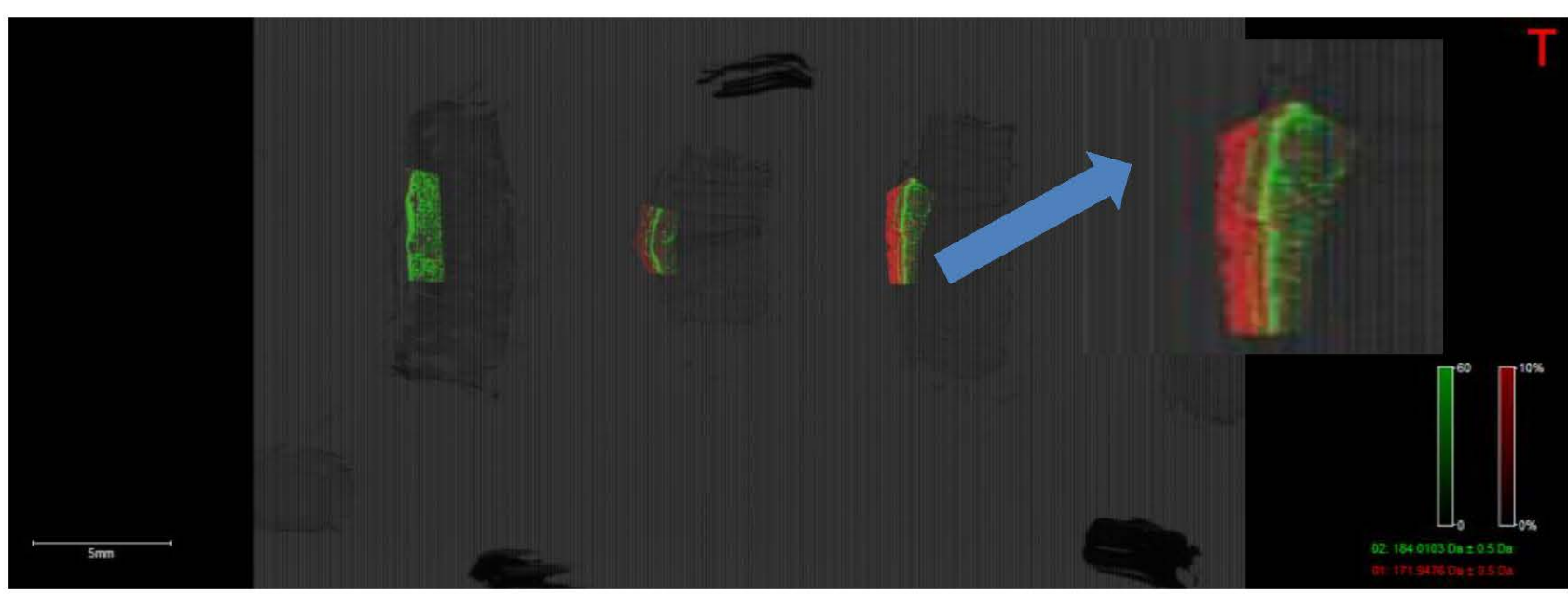


Figure 2: Optimised SB-MSI Experiment on Tolbutamide a CYP2C9 substrate (green) and PC Lipid Head Group (red) no evidence of metabolite formation was observed. Arrow indicates magnified image.

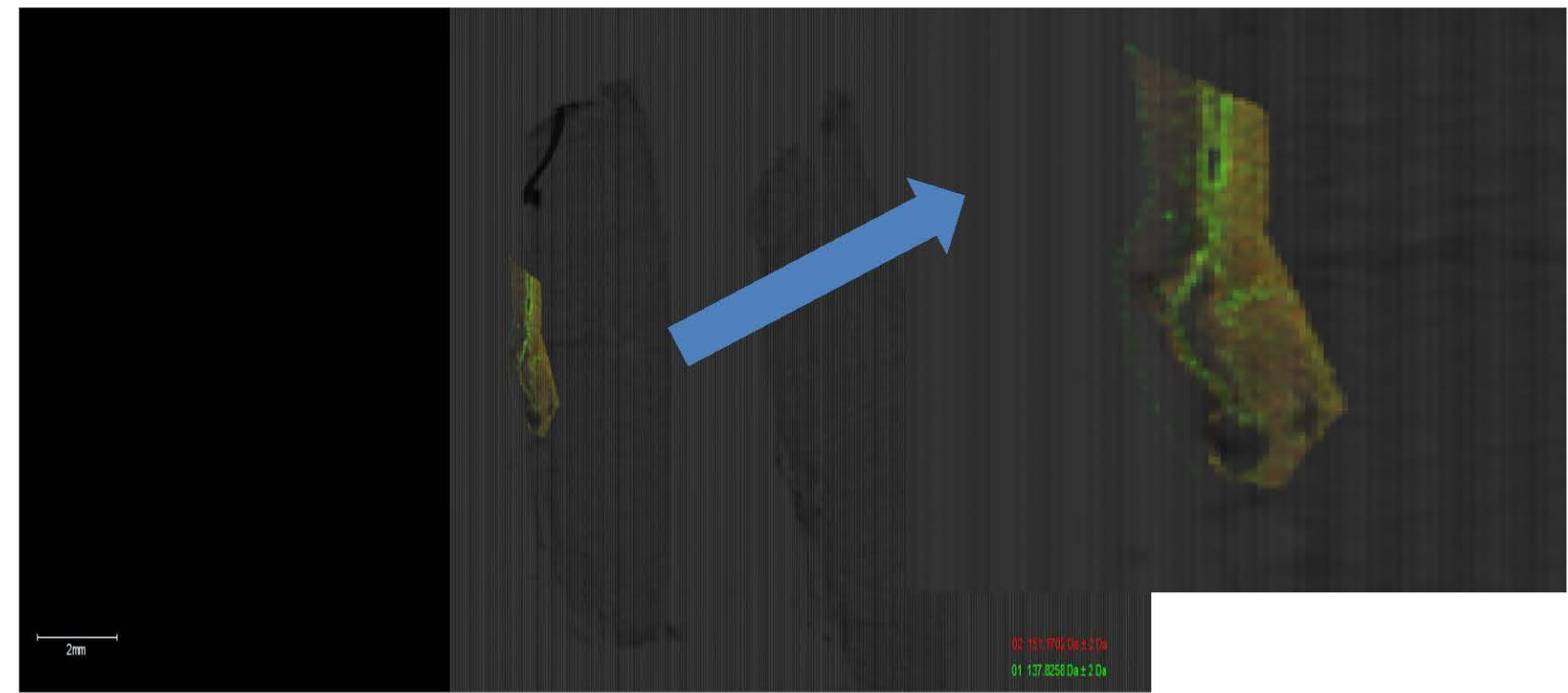


Figure 3: Optimised SB-MSI Analysis of Labskin treated with MethylParaben an esterase probe-Methyl paraben² (red) and p-hydroxybenzoic acid (green) overlay showing evidence of esterase activity which appears to be concentrated in a defined epidermal layer below the *stratum corneum*. Arrow indicates magnified image.

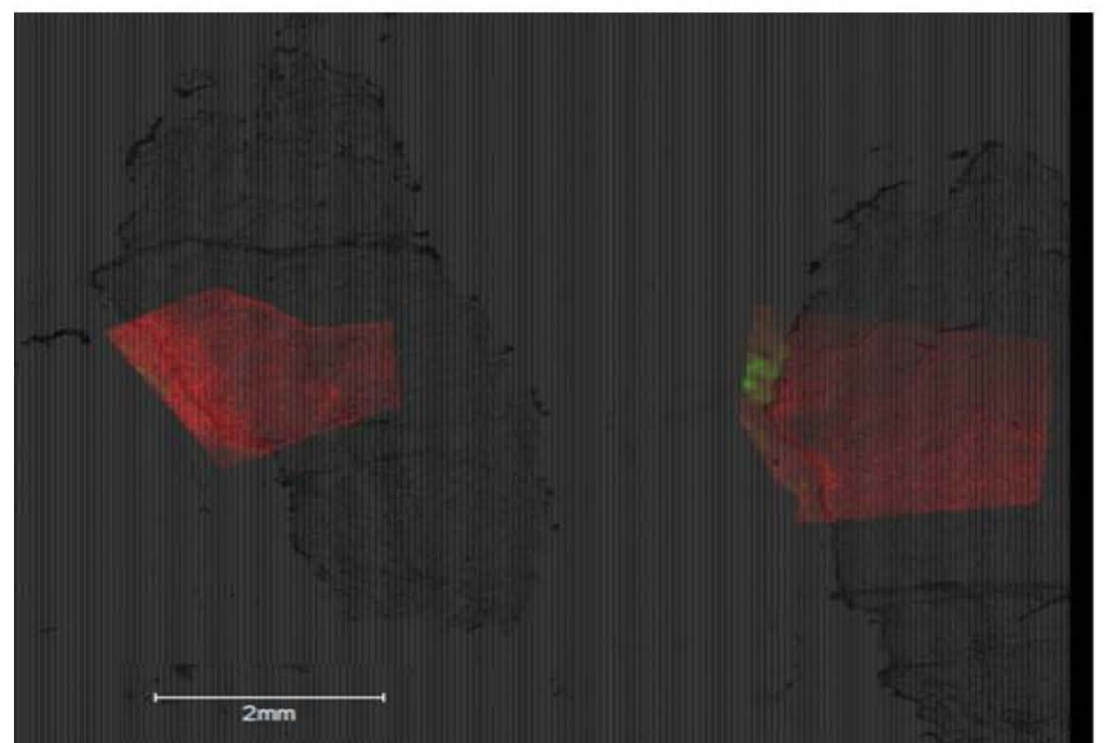


Figure 4: SB-MSI Analysis of Labskin treated with benzydamine a FMO probe: benzydamine (green) - Nor-benzydamine (red) possible evidence of low FMO activity throughout the epidermis.

Results and Discussion

In contrast to the major metabolising organ on the body the liver, no cytochrome P450s apart from P450 P8A1 (prostacyclin synthase) were detected in human skin microsomes (Table 1). Several non-P450 phase I XMEs were however expressed at detectable levels in skin microsomes (Table 2). Further analysis of the cytosolic fractions of two Labskin preparation and six human donor skin samples was made for soluble XMEs.

Although there was significant variation both between the two Labskin samples and across the different donor samples, consistent expression of several XMEs, representing both phase I (Table 1) and phase II (Table 2) metabolism, was noted in both the in vitro LSE model and in vivo samples. Furthermore, the soluble XME profile of the Labskin samples was remarkably consistent with the human skin samples.

In agreement with the proteomics data, SB-MSI showed no evidence of P450 like activity in the LSE for either of the two P450 probes Terbinafine and Tolbutamide (Figures 1 and 2 respectively). However, also in agreement with the proteomics data evidence for esterase activity was demonstrated for methyl-paraben (Figure 3). Some non-conclusive evidence for non-localised FMO activity for benzydiamine was also found (Figure 4) whereas this was not detected in the proteomics data. This was of note since FMO activity has been previously reported in both *ex-vivo* skin and LSE³.

Conclusions

- Untargeted proteomics analysis showed that human skin and a commercially available living skin equivalent model exhibited a similar distribution of xenobiotic metabolising enzymes.
- No P450s were found in either the human skin or the LSE but measurable levels of phase II enzymes, specifically esterases and GSTs were detected.
- The localisation of esterase activity was studied using a new technique: substrate based mass spectrometry imaging (SB-MSI).

References

- [1] van Eijl, S., Zhu, Z., Cupitt, J., Gierula, M., Götz, C., Fritsche, E., & Edwards, R. J. (2012). Elucidation of xenobiotic metabolism pathways in human skin and human skin models by proteomic profiling. *PloS One*, 7(7), e41721. doi:10.1371/journal.pone.0041721
- [2] Ford, G., McEwen, A.B., Wilson, K. and Wood, S.G. (2014) Metabolic transformations of alkyl parabens in the skin: Specific esterase inhibition study *Issues in Toxicology* 17-25.
- [3] Jäckh, C. *et al* (2011) Characterization of enzyme activities of Cytochrome P450 enzymes, Flavin-dependent monooxygenases, N-acetyltransferases and UDP-glucuronyltransferases in human reconstructed epidermis and full-thickness skin models. *Toxicology in Vitro* 25, 1209-1214.